ELSEVIER

International Journal of Heat and Fluid Flow 20 (1999) 470–476

International Journal of HEAT AND FLUID FLOW

www.elsevier.com/locate/ijhff

Dynamic processes occurring during the spreading of thin liquid films produced by drop impact on hot walls

Humberto Chaves *, Artur Michael Kubitzek, Frank Obermeier

TU Bergakademie Freiberg, D-09596 Freiberg, Germany

Abstract

When liquid drops impinge on a wall heated up above the boiling temperature of the liquid, bubbling and convection are observed in the emerging film which spreads along the wall. Experimental investigations of these processes and of the connected evaporation of the liquid are aimed at an improved understanding of the underlying mechanisms important for many technical applications. Typical Weber numbers of the impinging drops were varied between 50 and 700, the temperature of the polished aluminium wall between 70°C and 400°C, i.e., above the boiling temperature of ethanol used in the experiments. The growth rate of bubbles, their maximum diameter and their collapse as well as the formation and destruction of convection cells in the liquid film were recorded and analysed.

Notation

a	thermal conductivity
d	drop diameter
d_f	spreading diameter of the liquid film
g	acceleration due to gravity
h	film thickness
$h = (2/3)\ (d/d_f)^2 d$	estimated film thickness
$\mathrm{Ra} = g\beta(\Delta T)_h h^3/av$	Rayleigh number
T_B	boiling temperature
T_W	initial wall temperature
$(\Delta T)_h$	temperature difference between film surfaces
u	drop velocity before impact
$\mathrm{We} = \rho d u^2/\sigma$	Weber number
Greek	
β	thermal expansion coefficient
v	kinematic viscosity
ρ	density of the liquid
σ	surface tension of the liquid

1. Introduction

Dynamic processes occurring during the impact of drops on hot walls influence the heat transfer from the wall into the liquid and, thus, the total evaporation time of the liquid. A comprehensive understanding of these processes is important for technical application such as spray cooling (Mizikar, 1970), combustion (Arcoumanis and Chang, 1993), fire fighting (Ko and Chung, 1996), etc.

At the very beginning of the impact of drops on a hot surface they deform or spread forming a thin liquid film. Next, depending on conditions such as wall temperature and impact Weber number the film either contracts back into a drop, which can rebound, or the film breaks up into small ligaments and/or secondary droplets. These processes are accompanied by the evaporation of the liquid. Up to now, mainly isolated aspects of these phenomena were investigated experimentally as well as theoretically, e.g., the spreading process (Fukai et al., 1993), the rebounding process (Fujimoto and Hatta, 1996), the wettability of the surface (Nigmatulin et al., 1993), the evaporation of sessile drops (Mills and Fry, 1982; Wachters and Westerling, 1966), the transient wall temperature profile (Seki et al., 1978), and the heat transfer during the impact (Labeish, 1994; Takeuchi et al., 1983). Phenomenological studies of these phenomena have disclosed several different regimes of fragmentation (Bernardin et al., 1997; Jonas, 1996; Jonas et al., 1997; Kubitzek, 1997). Numerical models, which are based on empirical results, presently allow to calculate the dynamics of a spreading drop, Fukai et al. (1995) and to predict the heat transfer at low impact Weber number, Healy et al. (1998) in a temperature region where the liquid hovers on a steam cushion and does not touch the hot wall.

The present paper is directed to the investigation of the formation, the growth and the collapse of bubbles and convection cells within the thin liquid films, which are generated by drop impact normal to hot walls at high Weber number, and of their effects on the total evaporation of the liquid. High Weber numbers mean that the impact energy of the drop is chosen sufficiently large to cause spreading of the drop to a film in contrast to the phenomena observed for sessile drops at low Weber numbers <30. The results will be presented in the order as they occur in time, i.e. during early impact stages,

* Corresponding author. E-mail: hchaves@orion.hrz.tu-freiberg.de

0142-727X/99/$ – see front matter
PII: S0142-727X(99)00034-X

during spreading of the drop to form a film and late film boiling stages.

2. Experimental set-up

The experimental set-up shown in Fig. 1 can be subdivided into four components: the drop generation facility, the wall with its heating system, the picture acquisition, and the electronic control apparatus. The liquid was ethanol (surface tension $\sigma = 0.023$ N/m, density $\rho = 790$ kg/m^3), the wall an aluminium ingot with a polished surface whose roughness is less than 0.5 μm. The wall was heated electrically and PID controlled. The temperature of the wall was measured 1 mm below the surface of impact by means of a Ni–NiCr thermocouple with 1 K resolution. It was varied between $T_W = 79$°C and $T_W = 400$°C. For the majority of examples to be presented the velocities of the drops were $u = 0.93$, $u = 2.2$, $u = 3.36$ m/s and their diameter $d = 1.8$ mm, which imply Weber numbers We = 54, We = 300, and We = 700, respectively. The drops were generated by detachment from a teflon tube.

A photoelectric barrier passed by the drops produces a signal needed to trigger the acquisition apparatus. The time uncertainty was less than 300 μs mainly caused by a slight back and forth fluctuation of the droplet trajectories which cross the light barrier. All pictures were taken by CCD cameras. The temporal resolution of the highly reproducible phenomena could be realized by a time shift in the recording of single pictures from different impact events under the same conditions.

3. The formation and collapse of bubbles within the spreading film

In the temperature range between 79°C and 135°C, i.e., above the boiling temperature, a single bubble is observed at the impact centre which is due to air entrainment; in addition, a regularly distributed circle of bubbles occurs, Fig. 2(a). The latter are probably caused by a rarefaction wave within the drop which itself results from the reflection of the primary compression wave at the free surface of the impinging drop. Above a wall temperature of 135°C and up to 160°C an array of irregularly spaced bubbles appears, Fig. 2(b). It is well known that in this temperature range the roughness of the surface has a strong effect on nucleate boiling. At even higher wall temperatures, the bubbles coalesce and produce a steam layer between the drop and the wall, Fig. 2(c). Above $T_W = 400$°C, the cavities displays a ring structure around the impact centre, Fig. 2(d). It seems evident that they result from coalescing bubbles of a primary bubble ring created in the early stage of impact. Fig. 3(a)–(d) displays bubbles in the spreading liquid film for increasing wall temperatures 3 ms after the impact.

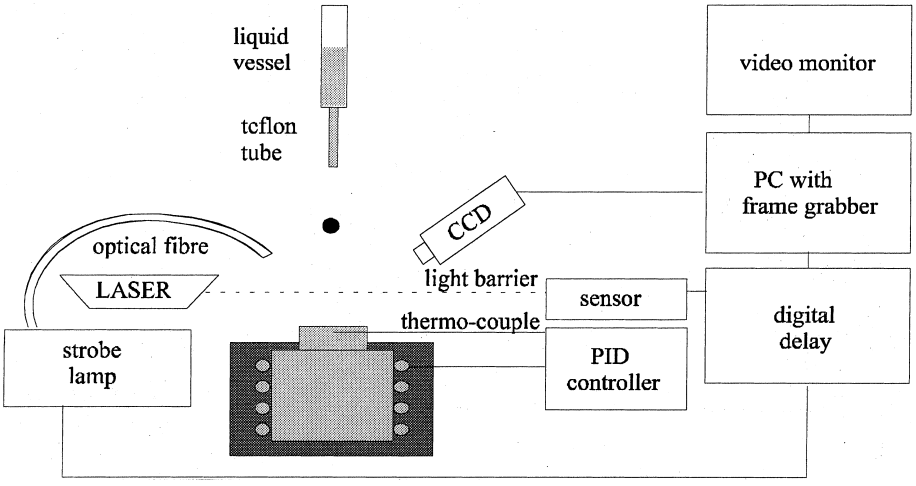

Fig. 1. Experimental set-up.

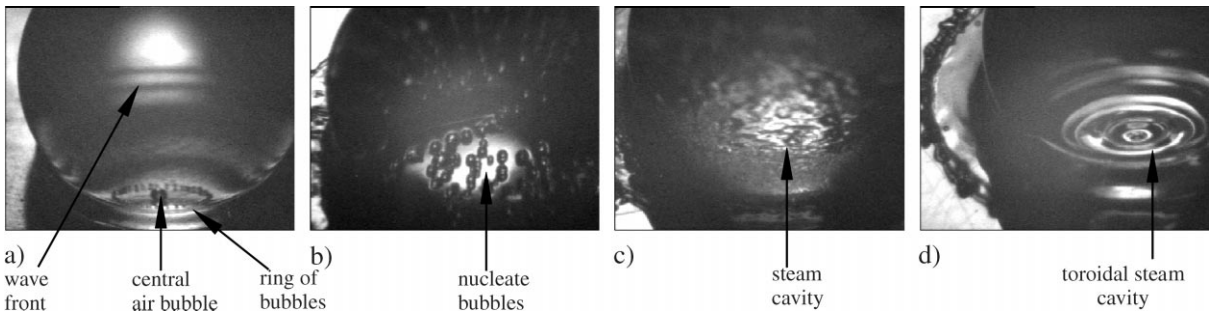

Fig. 2. Steam cavities or bubbles close to the liquid–wall interface at the beginning of the spreading of drops, $t<1$ ms, We = 300, (a) $T_W = 110$°C, (b) $T_W = 135$°C, (c) $T_W = 200$°C, (d) $T_W = 400$°C.

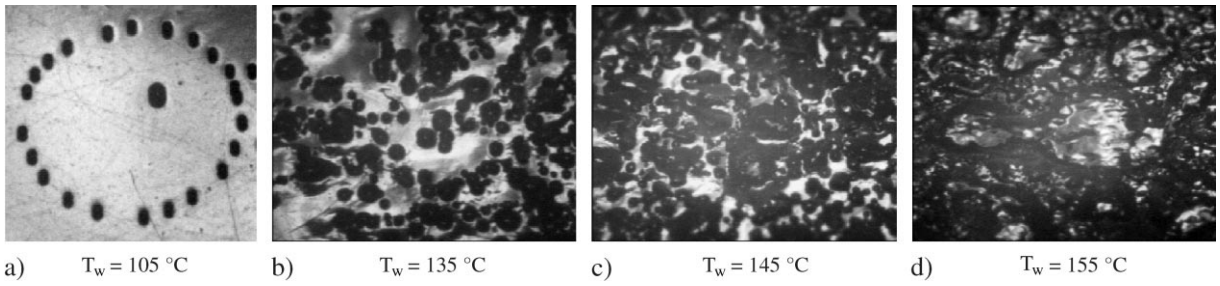

Fig. 3. Bubble arrays and steam cavities in the developed liquid film, $t = 3$ ms, We = 300.

The growth of the bubbles of the ring was measured, small bubbles grow approximately linearly with time. From the increase of the bubble diameter with time the velocity of the bubble growth could be calculated for different Weber numbers and different wall temperatures T_W, typical values are shown in Fig. 4.

The growth velocity of the ring bubbles does not depend on the Weber number. The maximum diameter, which these bubbles can attain, is limited. The bubbles either collapse or coalesce with each other. The maximum bubble diameter depends on the Weber number and on the wall temperature (Fig. 5). This outcome may be explained in the following way: During spreading of a drop the film diameter increases with time and reaches a maximal diameter before it starts to contract at low wall temperatures or it breaks up into small droplets at higher wall temperatures. With increasing Weber numbers the maximal film diameter increases thus producing thinner films. A bubble contained in the film can only reach a size which correlates with the film thickness. In Fig. 6(a) the variation of the maximal film diameter with the wall temperature is shown for different Weber numbers. Note that the realistic liquid film rim has a toroidal form, Fig. 6(b). The line named 'lift-off temperature' defines a temperature above which the liquid film does no longer touch the wall during the spreading process, it is characterized by film boiling. Between the boiling temperature and the lift-off temperature a characteristic variation of the maximum film diameter as a function of Weber number is observed. This variation is probably caused by the different importance of friction, surface tension, and inertia effects. However, the main effect of the Weber number is to distribute the liquid on a larger wall area enhancing heat transport from the wall.

The lift-off temperature varies with the Weber number. This is a consequence of the locally (and material) dependent heat transfer during the impact of the drops and the formation of the spreading film (Jonas et al., 1997). In the limit of low Weber numbers it corresponds to the Leidenfrost temperature for a sessile drop. It has been given a different name because it depends on the impact Weber number.

The bubbles life time after drop impact again depends on the Weber number and wall temperature, demonstrated in Fig. 7(a). For times above the drawn lines bubbles collapse. Collapsing bubbles can be seen in Fig. 7(b).

A schematic drawing shows details of the collapse of the bubbles in Fig. 8. As soon as a bubble reaches the free liquid surface, the thin liquid layer separating the steam within the bubble and the surrounding air ruptures. Next, the adjacent liquid starts to close the cavity and steam is discharged. Along the bubble axis perpendicular to the surface the liquid rises and forms a jet from which droplets can separate. This jet is called Rayleigh jet in splashing literature. With increasing wall temperature the length of the jet and the number of droplets increase. Additionally, circular waves propagate outwards from the centre of collapse and interfere, Fig. 9. At low wall temperatures the number of bubbles collapsing is relatively small and have therefore little effect on the mass and heat transfer of the film.

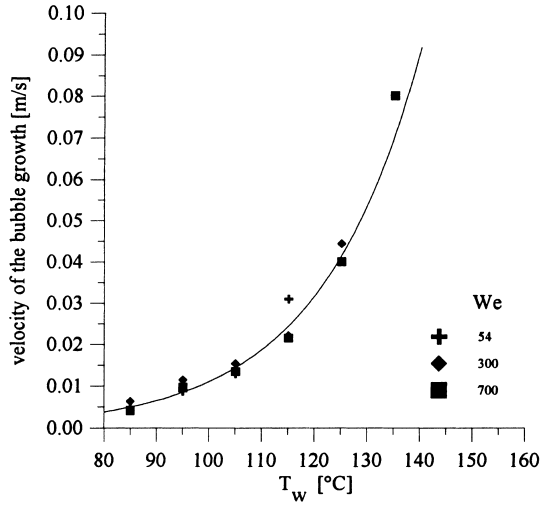

Fig. 4. Velocity of the bubble growth.

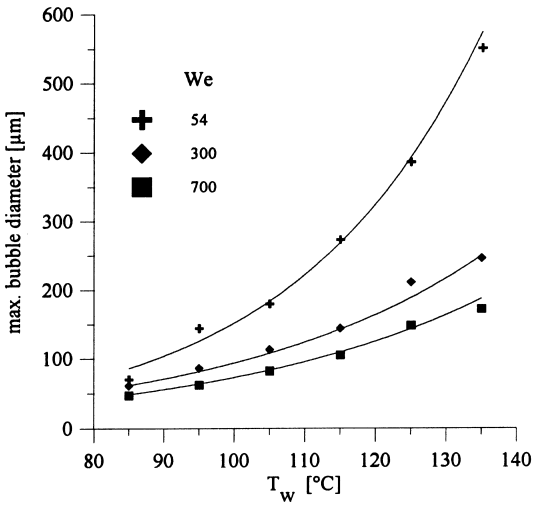

Fig. 5. Maximum bubble diameter before collapse.

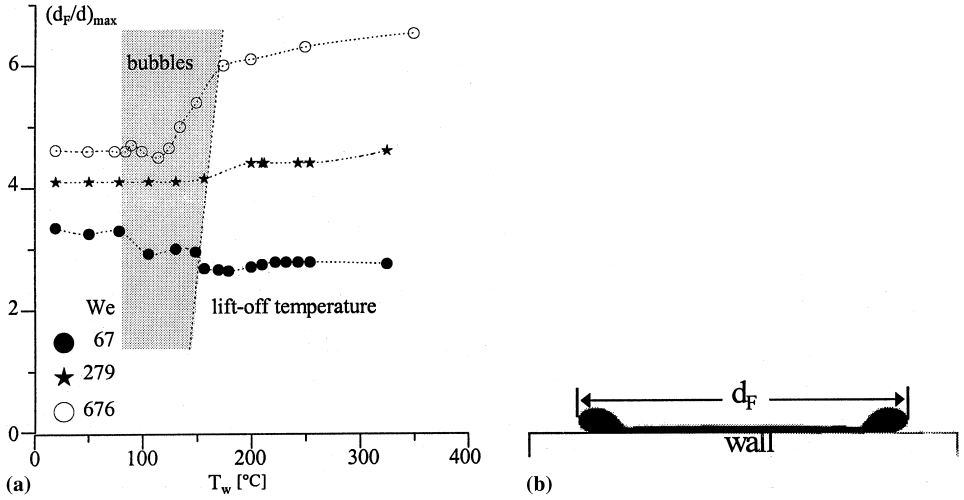

Fig. 6. (a) Maximum film diameter, grey area: bubble occurrence, (b) illustration of the cross-section of a realistic liquid film.

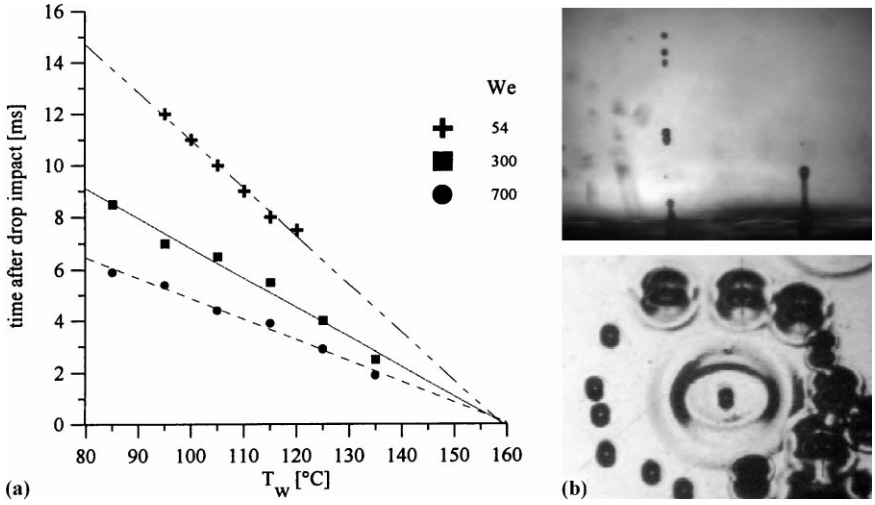

Fig. 7. (a) The limitation of the life time of the bubbles, (b) typical exposures of collapsing bubbles taken at two different viewing angles relative to the impact surface.

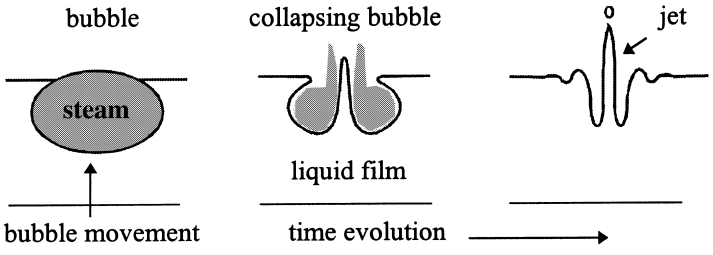

Fig. 8. Illustration of bubble collapse.

Moreover, in the temperature range between 135°C and 160°C, where the number of bubbles increases, the spreading fluid atomizes and produces a lot of tiny droplets and larger fragments close to the wall, Fig. 10. This powerful process, named miniaturisation by Inada and Yang (1993), corresponds to an immense increase of the free surface of the liquid and, therefore, to a decrease of the evaporation time.

4. Convection cells and break-up of the liquid film

For Weber numbers higher than 300 and wall temperatures above 200°C polygonial structures were observed on the film. They are the result of Rayleigh–Bernard convection in the fluid. These cell structures were observed when the film diameter is shrinking after having reached its maximum and is

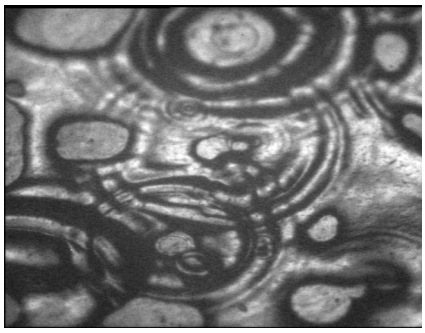

Fig. 9. Interfering waves after bubble collapse.

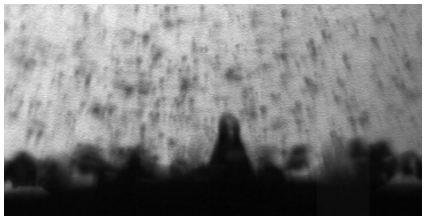

Fig. 10. Fluid miniaturisation; $T_W = 135°C$, $We = 85$.

still 2 to 3 times larger than the drop diameter. This corresponds to a film thickness of about 300 μm which can be estimated from the spreading diameter by equating the drop volume with a cylinder volume. An estimate of the Rayleigh number, $Ra = g\beta(\Delta T)_h h^3/av$, determined with thermal conductivity $a = 67.6e{-}9$ m^2/s, gravity $g = 9.81$ m/s^2, thermal expansion coefficient $\beta = 1.4e{-}3$ K^{-1}, kinematic viscosity $v = 0.566e{-}6$ m^2/s, and temperature difference between film surfaces $(\Delta T)_h = 59$ K for different liquid film thicknesses h is plotted in Fig. 11(a). The sketch, Fig. 11(b), shows the different layers affecting the convection. Note that the Rayleigh number is here proportional to the third power of the film thickness! The critical Rayleigh number $Ra_c = 657$ resulting from the stability analysis of a liquid film with two free surfaces (Merker, 1987) is the limit above which convection cells appear, this region is emphasized by a gray area in the plot.

The time evolution of these convection cells is presented in frames of Fig. 12. With increasing wall temperatures equivalent to the increasing temperature difference between the free film surfaces and the wall, the cell size decreases and the structure becomes more irregular.

The observed convection cells have a typical length scale between 100 and 200 μm, Fig. 12(a), with progressing time these cells become more pronounced, Fig. 12(b). Then the edges grow in such a way that the cells shrink and the cells start to crack in times less than 200 μs, Fig. 12(c). This fast process of the disruption of a cell is documented in a series of pictures, Fig. 13(a)–(c).

The mechanism of disruption is illustrated schematically in cross-sectional view of the fluid film, Fig. 14. The convection rolls in the liquid film lead to the formation of thin liquid bridges around the cells. When the film reaches a characteristic thickness these liquid bridges break leaving tiny bridge droplets behind. At the locations, where the edges of neighbouring cells meet, the liquid bridges are more stable than elsewhere. This observation results in the creation of mesh like pattern, shown in Fig. 15.

Also this intermediate state terminates very quickly. The connected ligaments tear at their knots and contract to droplets. Then these droplets move away from the hot surface and collect in a well defined region above the wall. A most likely reason for this movement is a collective Leidenfrost effect. For a given Weber number the upper limit of levitation as a function of time is shown in Fig. 16(a), a typical frame in Fig. 16(b). The gray area characterizes the transition time between the spreading and fragmentation of the drop and the subsequent movement of droplets and their evaporation. Its width marks approximately the uncertainties connected with the starting point of the levitation of droplets. Finally, it was observed that with increasing Weber number the transition occurs at earlier times after drop impact and that the droplets are smaller due to the initially smaller cells. Consequently, the evaporation rate is enhanced with increasing Weber number.

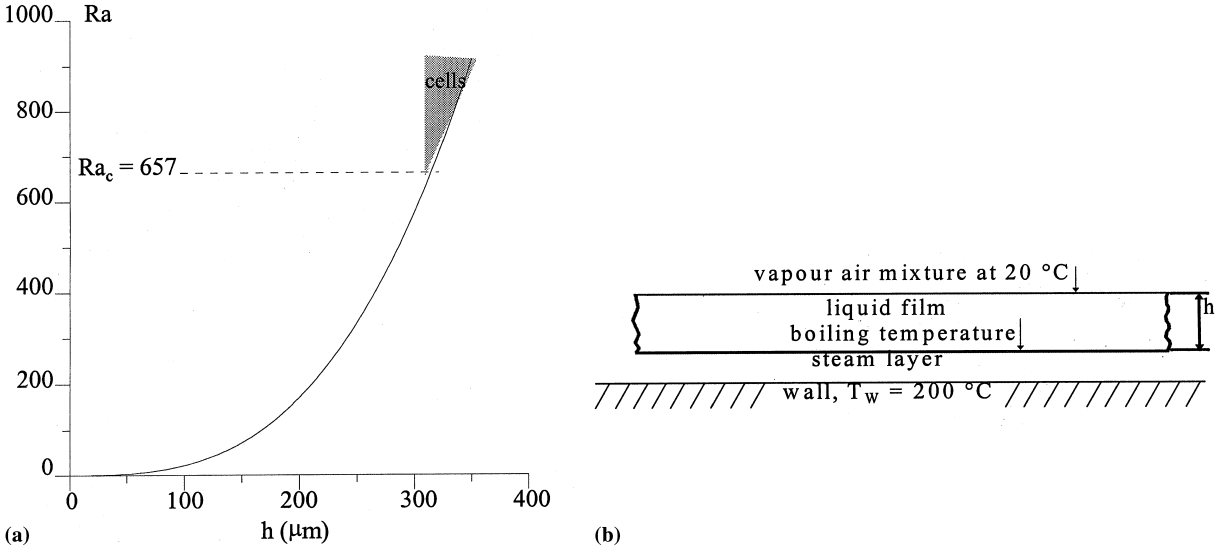

Fig. 11. (a) Appearance of convection cells in the liquid film, (b) illustration of the layers affecting the convection.

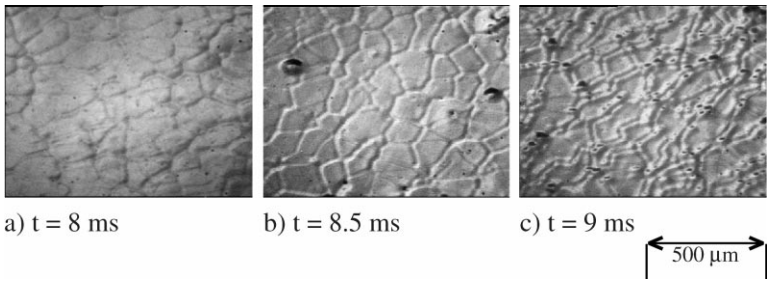

Fig. 12. Evolution of convection cells in a spreading liquid film after drop impact; We = 300, T_W = 200°C.

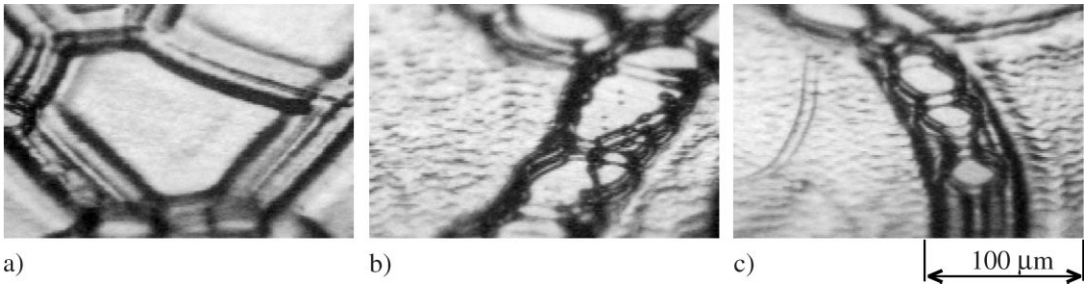

Fig. 13. (a) Convection cells, (b) and (c) break-up process of the cells edges; We = 300, T_W = 200°C.

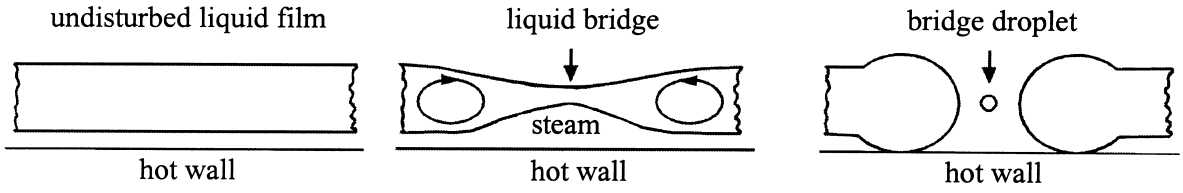

Fig. 14. Illustration of the liquid film disruption.

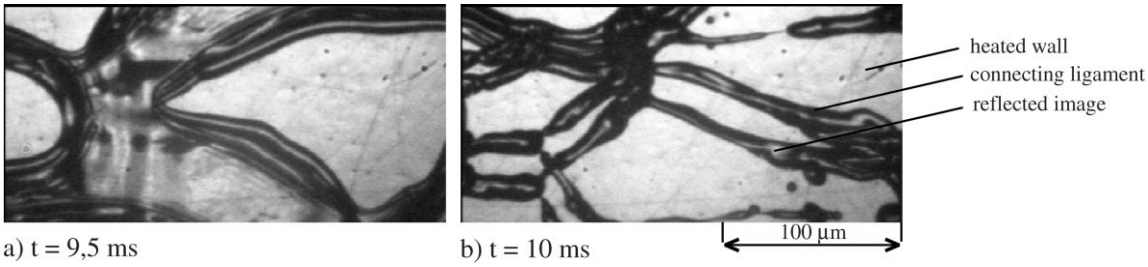

Fig. 15. (a) Shrinking of the liquid film, (b) formation of the mesh structures, We = 300, T_W = 400°C.

5. Conclusion

The dynamical processes of bubbling and convection within spreading ethanol films on hot walls, where the film is due to the impact of a drop, were studied. At wall temperature between 79°C and 135°C the formation of bubbles in the spreading fluid is observed. The velocity of the bubble growth is independent of the Weber number and depends on the wall temperature only. The maximum diameter, which a bubble reaches before collapsing, depends on both parameters. The collapsing bubbles are responsible for miniaturisation of the liquid and they determine the subsequent evaporation of the liquid. Above We_T = 300 and T_w = 200°C hexagonal convection cells in the liquid film occur. These structures disrupt at their edges and create a mesh like pattern. This is followed by the disintegration of the continuous liquid film and the formation of secondary droplets, which lift off from the surface and evaporate when hovering in a well defined region above the wall.

Acknowledgements

The present work was supported by the Deutsche Forschungsgemeinschaft as a project within the Schwerpunkt

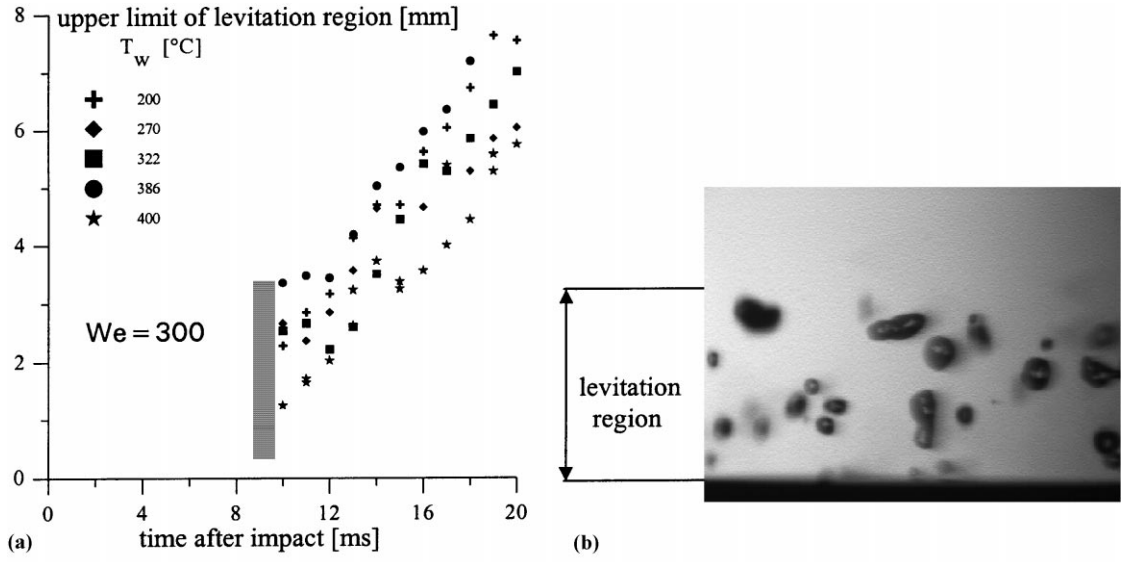

Fig. 16. (a) Upper limit of levitation region vs. time, (b) typical view of levitated droplets ensemble.

Programm SPP 725 'Transiente Vorgänge in mehrphasigen Systemen mit einer oder mehreren Komponenten'. We also acknowledge gratefully experimental contributions by T. Jonas.

References

Arcoumanis, C., Chang, J.C., 1993. Heat transfer between a heated plate and an impinging transient diesel spray. Experiments in Fluids 16, 105–119.

Bernardin, J.D., Stebbins, C.J., Mudawar, I., 1997. Mapping of impact and heat transfer regimes of water drops impinging on a polished surface. Int. J. Heat Mass Transfer 40, 247–267.

Fujimoto, H., Hatta, N., 1996. Deformation and rebounding processes of a water droplet impinging on a flat surface above Leidenfrost temperature. J. Fluids Eng. 118, 142–149.

Fukai, J. et al., 1993. Modelling of the deformation of a liquid droplet impinging upon a flat surface. Phys. Fluids A 5, 2588–2599.

Fukai, J., Shiiba, Y., Yamamoto, T., Miyatake, O., Poulikakos, D., Megaridis, C.M., Zhao, Z., 1995. Wetting effects on the spreading of a liquid droplet colliding with a flat surface. Experiment and modeling. Phys. Fluids 7, 236–247.

Healy, W.M., Halvorson, P.J., Hartley, J.G., Abdel-Khalik, S.I., 1998. A critical heat flux correlation for droplet impact cooling at low Weber numbers and various ambient pressures. Int. J. Heat Mass Transfer 41, 975–978.

Inada, S., Yang, W.J., 1993. Mechanisms of miniaturisation of sessile drops on a heated surface. Int. J. Heat Mass Transfer 36, 1505–1515.

Jonas, T., 1996. Transiente Phänomene beim Tropfenaufprall auf temperierte Wände. Diplomathesis, Georg-August-Universität, Göttingen, Germany.

Jonas, T., Kubitzek, A., Obermeier, F., 1997. Transient heat transfer and break-up mechanisms of drops impinging on heated walls. In: Proceedings of the Fourth World Conference on Experimental Heat Transfer, Fluid Mechanics and Thermodynamics, Brussels, pp. 1263–1270.

Ko, Y.S., Chung, S.H., 1996. An experiment on the break-up of impinging droplets on a hot surface. Experiments in Fluids 21, 118–123.

Kubitzek, A.M., 1997. Experimentelle Untersuchungen des Phasenübergangs beim Tropfenaufprall auf heiße Wände. Forschungsbericht 97–21 der Deutschen Forschungsanstalt für Luft- und Raumfahrt e.V., Germany.

Labeish, V.G., 1994. Thermohydrodynamic study of a drop impact against a heated surface. Experimental Thermal and Fluid Science 8, 181–199.

Merker, G.P., 1987. Konvektive Wärmeübertragung. Springer, Berlin, pp. 360–369.

Mills, A.A., Fry, J.D., 1982. Rate of evaporation of hydrocarbons from a hot surface: Nukiyama and Leidenfrost temperatures. Eur. J. Phys. 3, 152–154.

Mizikar, E.A., 1970. Spray cooling investigation for continuous casting of billets and blooms, Iron and Steel Engineer, June 1970, pp. 56–60.

Nigmatulin, B.I., Vasiliev, N.I., Guguchkin, V.V., 1993. Interaction between liquid droplets and heated surface. Wärme-und Stoffübertragung 28, 313–319.

Seki, M., Kawamura, H., Sanokawa, K., 1978. Transient temperature profile of a hot wall due to an impinging liquid droplet. J. Heat Transfer 100, 167–169.

Takeuchi, K., Senda, J., Yamada, K., 1983. Heat transfer characteristics and the breakup behaviour of small droplets impinging upon a hot surface. In: ASME–JSME Thermal Engineering Joint Conference, pp. 165–172.

Wachters, L.J.J., Westerling, N.A.J., 1966. The heat transfer from a hot wall to impinging water drops in the spheroidal state. Chemical Eng. Sci. 21, 1047–1056.